Received: 3 April 2020 | Revised: 20 September 2020 | Accepted: 29 September 2020

DOI: 10.1111/vsu.13531

ORIGINAL ARTICLE - RESEARCH

WILEY

A three-dimensional computed tomographic volume rendering methodology to measure the tibial torsion angle in dogs

Federico Longo DVM, PhD[1] | **Tommaso Nicetto DVM, PhD**[2] | **Antonio Pozzi DVM, ACVS, ECVS, ACVSMR**[1] | **Barbara Contiero MsS**[3] | **Maurizio Isola DVM, PhD**[3]

[1]Department of Small Animal Surgery, Vetsuisse Faculty University of Zurich, Zurich, Switzerland

[2]Diagnostica piccoli animali - Clinica veterinaria Pedrani, Vicenza, Italy

[3]Department of Animal Medicine, Productions and Health, University of Padova, Legnaro, Italy

Correspondence
Federico Longo, Department of Small Animal Surgery, Vetsuisse Faculty University of Zurich, Winterthurerstrasse 260, 8057 Zurich, Switzerland.
Email: federico.longo2@uzh.ch

Abstract

Objective: To describe a three-dimensional (3D) computed tomographic (CT) methodology to measure the tibial torsion angle (TTa) and to evaluate intrarater and interrater agreements and accuracy through comparison with anatomic measurements.

Study design: Ex vivo cadaveric study.

Sample population: Thirty-six tibiae from 18 dogs.

Methods: Tibial torsion angle of each tibia was measured by using two CT techniques (axial and 3D volume rendering) by three raters who blindly measured TTa in duplicate. A semitransparent bone filter was used to enhance the visibility of the target anatomical landmarks for the 3D volume rendering CT technique. Tibial torsion angle was also quantitated in tibial specimens. Intrarater and interrater agreements were analyzed by using intraclass coefficients (ICC). Accuracy was evaluated by using adjusted R^2 coefficients ($R^2 > 80\%$ was considered acceptable).

Results: The 3D volume rendering CT technique had excellent intrarater and interrater agreements (ICC > 0.94) and an R^2 value of 97%. The axial CT technique had good to excellent intrarater and interrater agreements ($0.8 < ICC < 0.95$) and an R^2 of 86%. No difference was found between axial and 3D CT techniques. A mean internal TT angle of approximately −6° was found with CT and anatomic measurements.

Conclusion: The 3D volume rendering and axial CT techniques were precise and accurate for measuring TTa in dogs unaffected by patellar luxation.

Clinical relevance: Combining 3D bone manipulation with application of a semitransparent filter allows simultaneous visualization of anatomic landmarks, which may facilitate the evaluation of complex bone deformations. Internal tibial torsion may be present in nonchondrodystrophic dogs without patella luxation.

1 | INTRODUCTION

Angular limb deformities may result from abnormal physeal growth,[1,2] congenital malformations,[1-4] dietary or hormonal causes, [3-5] or bone malalignment secondary to fracture malunion.[6] Long bone deformities are broadly classified in frontal, sagittal, and axial plane deformities.[7-11] The terms *torsional* and *rotational deformities* are often erroneously used as synonyms. Torsion is an axial plane deformity defined as the twisting of a single bone unit in the transverse plane around its longitudinal axis.[2,12-14]

Rotation is a multiplanar deformity that involves at least two bone units, has a pivot point in the joint, and is defined as an angulation around an axial or longitudinal axis.[2] From an anatomical perspective, tibial torsion (TT) is expressed as an external or internal torsion of the distal tibial epiphysis relative to the proximal tibial epiphysis.[13,15,16] Abnormal TT has been proposed as an etiopathogenic factor that may predispose to patella instability and osteoarthritis of the stifle in dogs.[17-19] Tibial torsion was detected in grade IV patella luxation cases along with concurrent complex skeletal malformations such as femoral frontal and axial malalignment,[8,17] metatarsal rotation, and pes deviation.[20] An accurate method to evaluate and quantify TT would be beneficial when complex hind limb deformities are evaluated, especially for planning surgical corrections.

In human medicine, different diagnostic approaches such as clinical examination,[16,21] radiography,[13,22] computed tomography (CT),[12,23-25] ultrasound,[26] and fluoroscopy[15,27] have been described for assessing TT. The accuracy of radiography[18] and CT[28] have been investigated in the first reports in veterinary medicine focusing on TT. The main finding highlighted in these reports is that radiography failed to discriminate between internal torsion and rotation,[18] whereas CT exhibited a satisfactory measurement accuracy.[28] Aper et al[28] described an axial CT assessment of TT in a group of medium to large mixed-breed dogs by using two different pairs of reference axes adapted from reports in the human literature.[16] Other researchers[19,29-31] investigated the TT using only one of the two pairs of axes proposed by Aper at al[28] in individual breeds. As a result, depending on the pair of axes used, different values were found, providing evidence of the presence of either external or internal TT in dogs.[19,28-30,32]

By reviewing the veterinary literature on TT, the authors found two main areas of interest for further investigation. First, the identification of the distal cranial tibial (CnT) axis was somewhat unclear because it was not defined in which CT slice of the distal tibial epiphysis the CnT axis should be drawn. Second, the direction of physiological TT (external or internal) in dogs unaffected by patella luxation was conflicting.[19,28,30,32] Furthermore, to the best of the authors' knowledge, no previous reports on tibial torsion describe the intrarater and interrater agreements for the measurement of TT angle (TTa).

Therefore, the threefold objective of this study was to (1) describe a three-dimensional (3D) volume rendering CT methodology for measuring TTa, (2) investigate its precision (intrarater and interrater agreement)[33,34] and accuracy (comparison with anatomic measurements), and (3) compare the 3D volume rendering and axial CT TTa measurements. The TTa was quantitated by using the proximal caudal tibial condylar (CdC) and the distal cranial CnT pair of axes.

Our hypotheses were that (1) a 3D volume rendering CT technique would be precise and accurate and (2) there would be a physiological internal TT in dogs not affected by patella luxation.

2 | MATERIALS AND METHODS

Canine tibiae were collected from client-owned dogs that had been euthanized for reasons unrelated to the present study, and the tibia specimens were enrolled under the condition of informed consent signed by the owners. Sex, age, weight, and breed were recorded. Medical record reviews, orthogonal radiographic surveys of the stifle and the tibia, and gross physical examinations of the fresh cadavers were performed to exclude the presence of patellar luxation and frontal plane deformities.

The cadavers were positioned on a foam cradle in dorsal recumbency with the hind limbs extended and the tibiae placed as parallel as possible to the CT table. Computed tomography of the whole hind limbs (from the ilial wing body to the metatarsus) was performed by using a 4-row multidetector CT scanner (Asteion S4; Toshiba Medical Systems Europe; Zoetermeer, the Netherlands) in helical acquisition mode with a slice thickness of 1 mm (reconstruction interval of 0.8 mm), with a distal-to-proximal scanning direction. Scans were reconstructed in DICOM (digital imaging and communications in medicine) software (Osirix, version 5.8, Pixmeo Sàrl; Bernex, Switzerland), which was also used for TTa measurements.

Three raters (F. L, T. N, M. I.) blindly measured TTa in duplicate with two different CT methodologies (axial and 3D volume rendering CT). The raters had different levels of experience in using the software (one professor of small animal orthopedics, one experienced orthopedic surgeon, and one low-experienced orthopedic surgeon).

To prevent any measurement conditioning, each CT was anonymized, labeled as “LT” (left tibia) or “RT”

(right tibia), and randomized with an open source program (Research Randomizer, version 4.0; https://www.randomizer.org/). An additional fourth examiner (no experience in orthopedic surgery) performed the TTa calculation in duplicate on digital images obtained from tibia specimens.

2.1 | Computed tomographic axial measurement of TTa

A methodology similar to that described by Aper et al[28] was used. First, the proximal axial CT slice, where the most caudal points of the tibial condyles were simultaneously identifiable, was selected (Figure 1A,D). Second, the most caudal points of the tibial condyles were aligned according to the horizontal toolbar provided by the DICOM software. The CdC axis was drawn as a line parallel to the caudal condylar tibial cortex (Figure 1A,D). The "propagate ROI" function was selected, so that the CdC remained visible while CT slices were being scrolled through. Third, the slice tracing the CnT axis was defined as the CT transverse section nearly proximal to the talocrural joint. Therefore, the distal tibial epiphyses, calcaneus, and lateral malleolus were all detectable (Figure 1B,E). Fourth, the CnT axis was drawn as the line passing through the most prominent points of the cranial tibial cortex (Figure 1B,E). Fifth, the TTa was directly measured by using the "Cobb angle function" (Figure 1C,F). When the vertex angle was directed medially, a negative value was assigned to the CdC/CnT angle (internal TT, Figure 1C), while a positive value (external TT) was

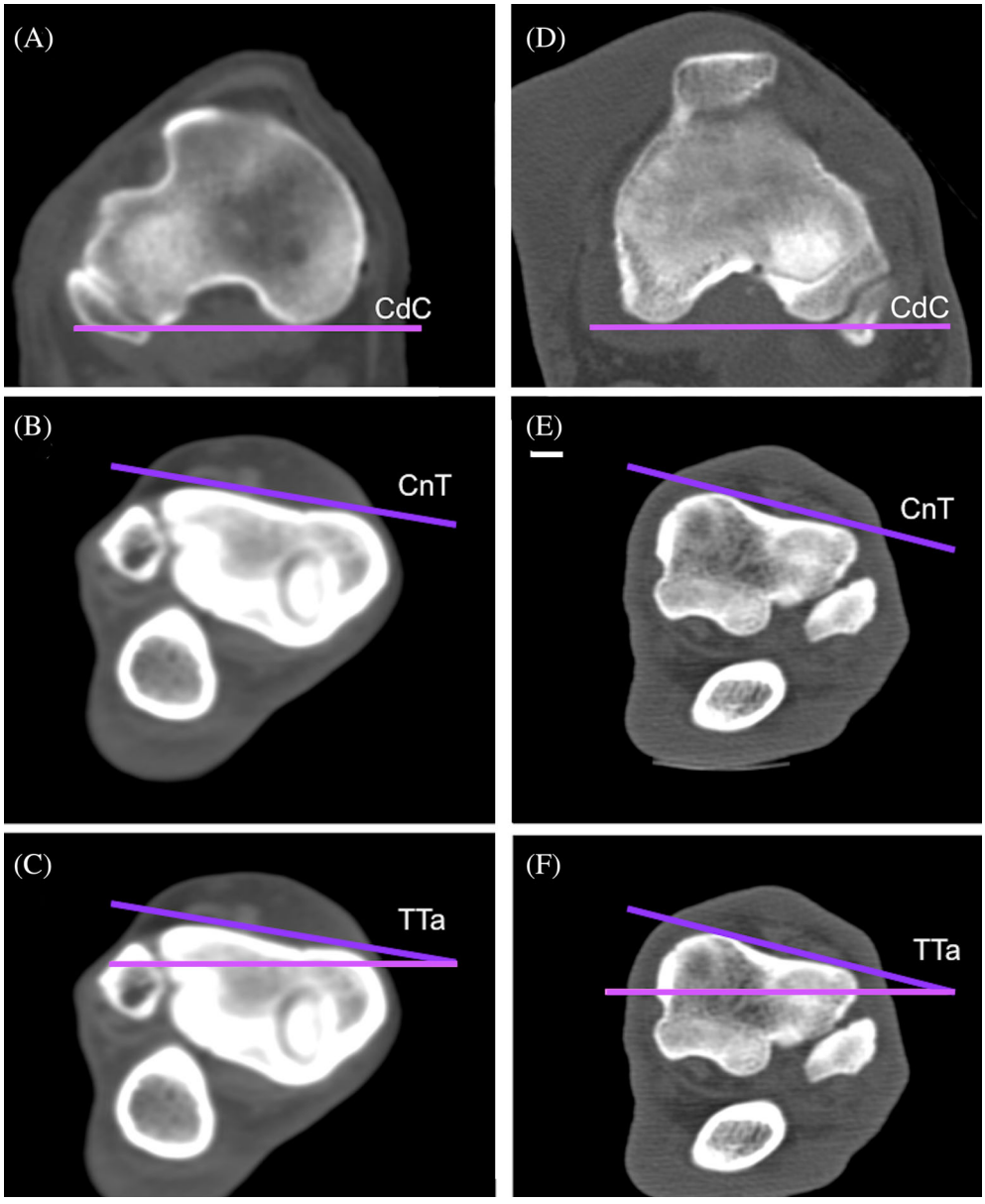

FIGURE 1 Evaluation of tibial torsion angle (TTa) by using an axial computed tomographic (CT) technique in a right tibia of a German shepherd (A-C) and a left tibia of a mixed breed dog (D-F). The CT slice in which the most caudal points of the proximal tibial epiphysis appeared was identified (A,D). The caudal condylar (CdC) axis was drawn as a line passing through the most caudal tibial points (pink line; A,D). A CT slice proximal to the talocrural joint was selected; the distal tibia, calcaneus, and lateral malleolus were all visible (B,E). The cranial tibial (CnT) axis was defined as a line passing through the most prominent points of the distal cranial cortex (purple line; B,E). The axial CT TTa was measured (C,F). An internal TT of −7° (C) and an external TT of 14° (F) were measured

assigned when the vertex of the TTa was lateral (Figure 1F).

2.2 | Three-dimensional volume rendering CT measurement of TTa

For performing the 3D volume rendering CT measurement of TTa, first, the multiplanar reconstruction (MPR) function was selected. Proximal and distal fiducial markers (green points in Figure 2) were positioned on the target tibia by using the reference proximal and distal landmarks of the mechanical tibial axis.[35] Therefore, the proximal point was centered between the intercondylar tubercles, whereas the distal point was positioned on the craniodistal intermediate ridge of the tibia (Figure 2A).[35] Second, the 3D volume rendering function was selected. The tibia was isolated from the femur and metatarsus. A medial sagittal view was used to detect the most caudal point of the medial tibial condyle (Figure 2B). The proximal tibial epiphysis was then slightly externally rotated to visualize the most caudal point of the lateral tibial

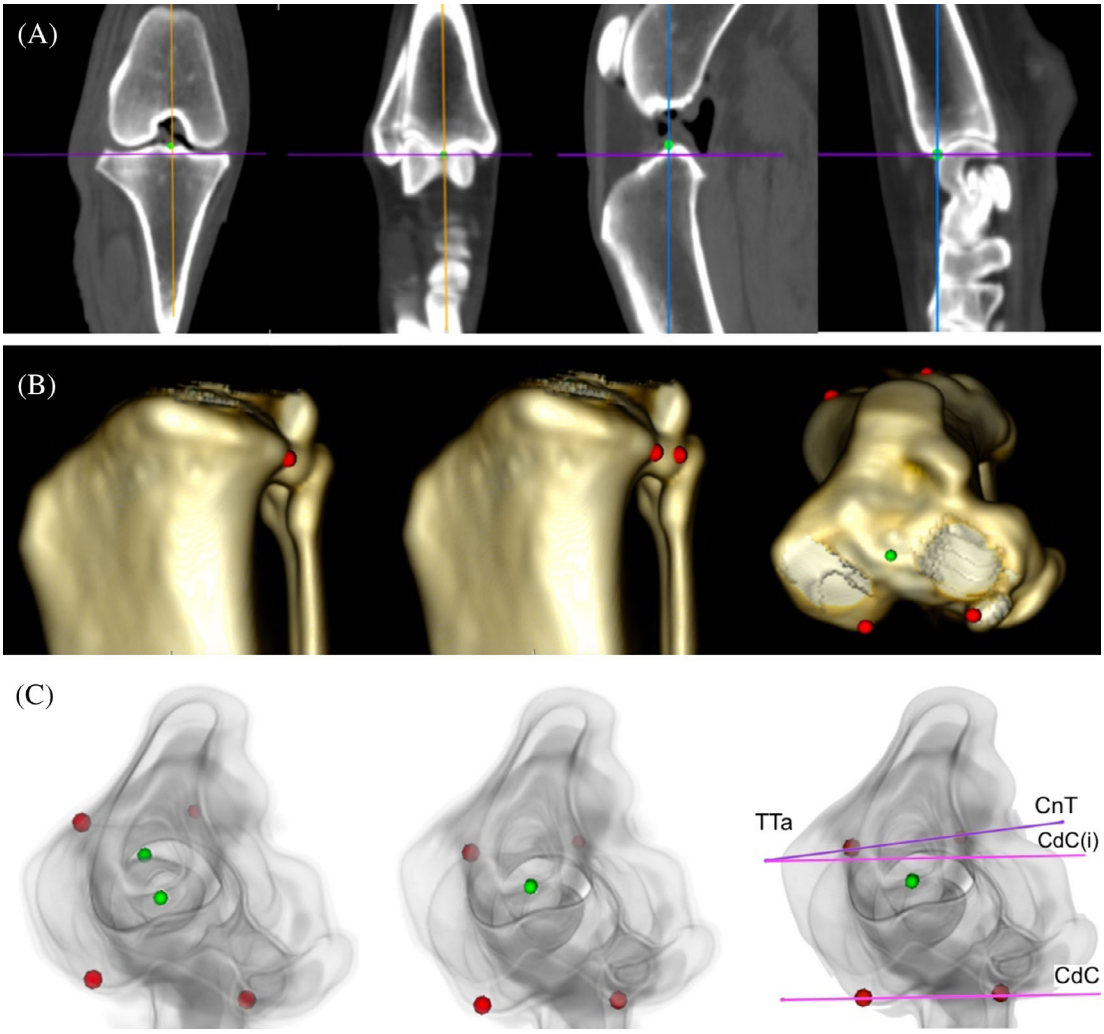

FIGURE 2 Evaluation of tibial torsion angle (TTa) by using a three-dimensional volume-rendering computed tomography (3D CT) technique in a right tibia of a German shepherd. The multiplanar reconstruction (MPR) function was selected. The proximal and distal tibial landmarks required to draw the mechanical tibial axis were found: MPR frontal and medial views (A). The target tibia was cropped from the femur and metatarsus. A sagittal medial view of the tibia was used to identify the most caudal point of the medial tibial condyle (B, image at left). The tibia was slightly externally rotated to visualize the most caudal point of the lateral tibial condyle (B, central image). The most prominent points of the distal cranial tibial cortex were marked. The tibia was positioned in the axial plane but in proximal-to-distal direction (B, image at right). A semitransparent bone filter was used to achieve sufficient transparency to simultaneously evaluate the proximal and distal tibial epiphyses (C, image at left). The proximal and distal points for the mechanical axis projection were superimposed (C, central image). The caudal condylar (CdC; pink line) and cranial tibial (CnT; purple line) axes were drawn, and the TTa was calculated (C, image at right)

condyle. Third, a distal-to-proximal axial tibial view was used to identify the most prominent points of the distal cranial tibial cortex. The tibia was thereafter positioned in the opposite direction (proximal-to-distal; Figure 2B). Fourth, a semitransparent bone filter (dark bone filter, 4) was applied. The histogram that routinely appears in the chromatic toolbar was adjusted by shadowing the surrounding soft tissues and increasing the bone transparency. As a result, the proximal and distal cortical profiles of the tibial epiphyses were visible as well as the intramedullary tibial canal (Figure 2C). Fifth, the proximal and distal fiducial markers, simulating the mechanical axis of the tibia, were superimposed (Figure 2C). Sixth, the 3D reconstructed image was saved as a DICOM file. The CdC and CnT axes were drawn on the axial 2D image, and the TTa was measured by using the Cobb function (Figure 2C). The same criterion previously described for axial CT was used to attribute negative and positive values to the TTa.

2.3 | Anatomic measurements

Every tibia was disarticulated and placed on a plexiglass support. The tibial diaphysis was slightly elevated by using a sponge material to ensure that the caudal aspects of the tibial condyles were touching the plexiglass plane and the cranial cortex of distal tibia was partially visible. Proximal and distal Kirschner wires, fixed onto the bone with glue, were used to mimic the orientation of the CnT and CdC axes (Figure 3A,B). Digital images were obtained in a proximal-to-distal direction (axial view) with a predetermined digital camera lens-to-bone distance. An additional examiner measured the anatomic TTa in duplicate with the same DICOM software and Cobb angle function used by the three raters for CT measurements (Figure 3C).

2.4 | Statistical analysis

Three software packages (MedCalc version 17.3, MedCalc Software, Ostend, Belgium; SAS version 9.4, SAS Institute, Cary, NC; R package version 4.0.1, R Foundation for Statistical Computing, Vienna, Austria; https://www.r-project.org) were used. Data normality of all data sets was tested by using the Shapiro–Wilk test. The circular data of the TTa calculated with CT and anatomic methodologies (axial CT TT, 3D CT TT, and anatomic tibia torsion angle [A-TT]) were extrapolated by using a macro for circular data analysis (SAS code for circular statistics; www.researchgate.net/publication/269762898).

The precision (intrarater and interrater agreement) of the measurements was assessed by using intraclass coefficients (ICC) with 95% CI. An ICC <0.8 was considered fair, 0.8 to ≤0.9 was considered good, and > 0.9 was considered excellent.[33,34]

The adjusted R^2 was adopted to investigate the strength of agreement between the CT measurements (axial CT TTa and 3D volume rendering CT TTa) and anatomic measurement on tibial specimens (A-TT). Accuracy was considered acceptable when $R^2 > 80\%$.[28,36] An analysis of variance (ANOVA) model for circular data (R software package "circular"; R Foundation for Statistical Computing) was adopted to test the effect of the three methods (axial CT vs A-TT and 3D volume rendering CT vs A-TT). By using the same approach, the effect of the three raters for the two CT measurements (axial and 3D volume rendering CT) was assessed. Statistical significance was set at $P < .05$. A Bland–Altman plot was used to compare axial CT and 3D volume rendering CT

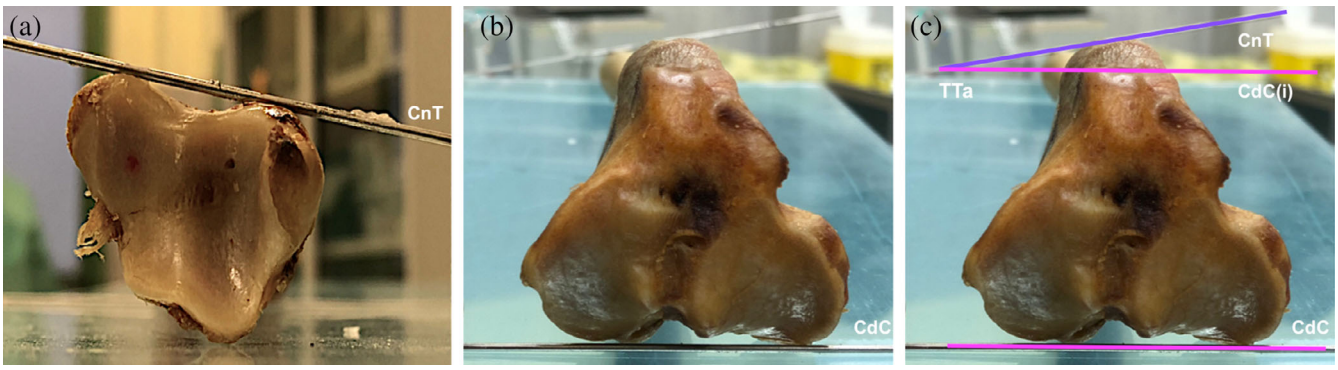

FIGURE 3 Anatomic measurement of tibial torsion angle (TTa). Each tibia specimen was positioned in a plexiglass support. Two Kirschner wires of an appropriate diameter were used to simulate the cranial tibial (CnT; A) and caudal condylar (CdC; B) axes. A digital image with a predetermined lens-to-bone distance was obtained in the proximal-to-distal direction (B). The CnT (C; purple line) and CdC (C; pink line) axes were superimposed onto the Kirschner wires. The TTa was quantitated (C)

measurements with the anatomic measurements. After referring to the literature that used the same pair of axes,[28,32] a calculation, based on the available sample size, of the statistical power of the test was conducted. A posteriori calculation of the sample dimension was performed by using the paired *t* test.

3 | RESULTS

Thirty-six tibiae obtained from 18 nonchondrodystrophic cadaver dogs were used, of which nine were female and nine were male. The mean age was 5.2 years (median, 6.7; range, 2.3-13). The mean body mass was 24.8 kg (median, 29.2; range, 19.3-39). The breeds used were German shepherd (5), mixed-breed dogs (4), Labrador retriever (4), Drahthaar (2), Dobermann (2), and Irish setter (1).

All the data met the normality assumption. Overall, there was good intrarater agreement for the axial CT technique (ICC = 0.87; Table 1) and an excellent intrarater agreement for the 3D volume rendering CT technique (ICC = 0.95; Table 1). The intrarater ICC for each rater are displayed in Table 1. The anatomical measurements were the most reproducible (ICC = 0.98). There was an overall excellent interrater agreement for both techniques (axial CT ICC, 0.91; 3D volume rendering CT ICC, 0.95; Table 2). All three raters exhibited good to excellent ICC in terms of either intrarater (Table 1) or interrater (Table 2) agreement. Rater 1 was the worst compared with raters 2 and 3. However, according to ANOVA, we did not find a rater effect within each CT technique (axial CT, $P = .940$; 3D CT, $P = .942$).

With regard to accuracy assessment, the adjusted R^2 values of both axial and 3D CT measurements were greater than the 80% threshold (Figure 4A, upper line). In detail, the axial CT R^2 was 86%, while the 3D volume rendering CT R^2 was 97%. The measurements were well aligned along the regression lines, most strongly for 3D volume rendering CT TT measurements (Figure 4A). The Bland–Altman plot (Figure 4B, bottom line) illustrated that less homogenous measurements were performed when $-5^\circ <$ TT angle $<0^\circ$ and $5^\circ <$ TT angle $<10^\circ$.

The 3D volume rendering CT technique exhibited a superior precision and was 10% more accurate compared with the axial CT technique. However, when the variances between the measurement averages of both CT techniques were compared, ANOVA results provided evidence that there was no difference between them ($P = .877$). Mean, SD, and median of TTa are presented in Table 3. A internal TT was found in all the specimens examined. Specifically, the anatomic TTa was -6° ($\pm 5.9^\circ$), the axial CT TTa -6.5° ($\pm 5.9^\circ$), and the 3D volume rendering CT TTa was -5.8° ($\pm 5.7^\circ$).

On the basis of the preliminary power analysis and after three potential scenarios were taken into consideration, the statistical power of the test was calculated by using a difference between CT and anatomic measurements equal to 3°, 3.5°, and 4°; an SD equal to 5.1°; and a type I error equal to 5%. The power of statistical test results were equal to 69%, 82% and 91%, respectively.

From the results obtained, a posteriori power analysis was performed. The paired difference between the two methods (anatomic and CT) was 0.25 ± 1.01. After a mean significant difference between anatomic and CT measurements equal to 0.5 and the SD of the difference between the two methods equal to 1.01 was considered, assuming a type 1 error equal to 0.05 and a power of 80%, the sample size requested for the paired samples *t* test was equal to 34.

4 | DISCUSSION

This ex vivo study describes the use of a 3D volume rendering CT function to quantitate TTa in medium to large nonchondrodystrophic dogs unaffected by patellar luxation.

Intrarater and interrater agreement was good, providing sufficient evidence for us to accept our first hypothesis. Furthermore, our findings provide evidence that the measurements performed on reconstructed CT images

TABLE 1 Intrarater ICC calculated for each rater with axial CT and 3D volume rendering CT techniques

Technique	$Intrarat_1$ ICC	$Intrarat_2$ ICC	$Intrarat_3$ ICC	$Intrarat_{1,2,3}$ ICC	$Intrarat_{Ex}$ ICC
Axial CT	0.80 (0.65-0.89)	0.92 (0.83-0.96)	0.90 (0.82-0.95)	0.87 (0.65-0.96)	...
3D CT	0.94 (0.88-0.96)	0.96 (0.93-0.98)	0.95 (0.91-0.97)	0.95 (0.88-0.98)	...
Anatomic	...	...	...	...	0.98 (0.97-0.99)

Note: Data are mean (95% CI).

Abbreviations: ..., not applicable; 3D, three dimensional; CT, computed tomography; Ex, additional examiner; ICC, intraclass correlation coefficient; Intrarat, intrarater.

TABLE 2 Interrater ICC calculated for each rater for axial CT and 3D volume rendering CT techniques

Technique	$Interrat_{1,2}$ ICC	$Interrat_{1,3}$ ICC	$Interrat_{2,3}$ ICC	$Interrat_{1,2,3}$ ICC
Axial CT	0.89 (0.80-0.94)	0.90 (0.81-0.94)	0.95 (0.91-0.97)	0.91 (0.80-0.97)
3D CT	0.96 (0.92-0.98)	0.95 (0.91-0.97)	0.96 (0.94-0.98)	0.95 (0.91-0.98)

Note: Data are mean (95% CI).
Abbreviations: 3D, three dimensional; CT, computed tomography; ICC, intraclass correlation coefficient; Interrat, interrater.

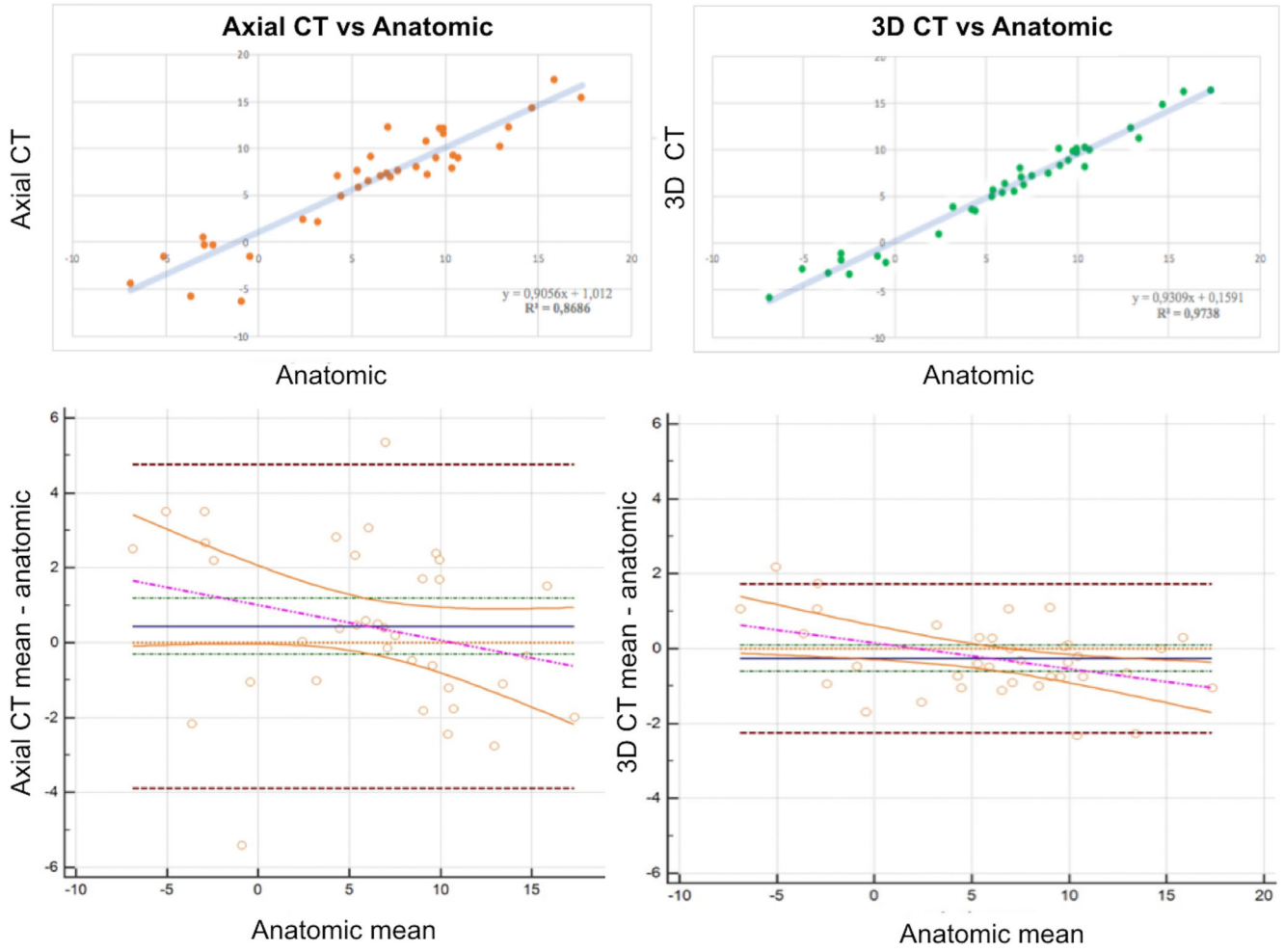

FIGURE 4 Graphical representation of regression line analysis (A) and Bland–Altman plot (B) for the comparison between the tested methods (axial and three-dimensional computed tomography [3D CT]) and the reference method (anatomic). A, The R^2 coefficient for both CT techniques is above 80%, with the 3D CT having superior accuracy (R^2 = 97%) compared with axial CT (R^2 = 86%). B, The axial CT technique (left plot) has wider lower and upper limits of agreement (dashed brown lines), a larger gap between the parallel line of the X axis (dashed yellow line) and mean line (continuous blue axis), and wider CI limits (continuous yellow lines) compared with the 3D CT technique. The dashed purple line represents the regression line

TABLE 3 TTa measured by the three raters and by the additional examiner for the anatomic specimens

TT angle	Rat_1	Rat_2	Rat_3	$Rat_{1,2,3}$	Examiner
Axial CT, °	−6.79 ± 5.95	−6.33 ± 6.10	−6.39 ± 5.84	−6.51 ± 5.97	...
3D CT, °	−5.96 ± 5.70	−5.92 ± 5.99	−5.53 ± 5.39	−5.80 ± 5.70	...
Anatomic, °	...	...	...	...	−6.05 ± 5.97

Note: Data are mean angle ± circular SD. Negative values = internal TT, and positive values = external TT.
Abbreviations: ..., not applicable; 3D, three dimensional; CT, computed tomography; Rat, rater; TT, tibial torsion; TTa, TT angle.

were similar to those derived from digital images obtained from tibia specimens (accuracy).

In this study, we used the same pair of axes (CdC/CnT) adopted by Aper et al[28] and Newmann et al.[32] We also assessed the precision for using this pair of axes because it had not been previously investigated.

Although the 3D volume rendering CT technique resulted in superior accuracy with more homogeneous measurements, the results provide evidence that the axial CT is also a reliable technique for measuring TTa. The CT axial technique exhibited good to excellent precision and good accuracy, and it was not significantly different compared with the 3D volume rendering CT technique. Therefore, we would support the use of both techniques for TT evaluation, having considered that the variable experience of the readers did not affect the results.

The accuracy is a statistical description of how close is a calculated value to an assumed true value, which implies that a "true" value must be both detectable and measurable.[34] In this study, we assumed the anatomical measurements as the gold standard method, as previously described.[28,35] To support this assumption, we assessed the intrarater agreement of anatomical measurements, and we found that they were the most repeatable measurements. This result was not unexpected because the reported benefits of an ex vivo measurement include the easy accessibility of bony landmarks to direct observation.[28] As a result, anatomical measurements historically provided the reference database for assessing angles and, thus, are referred to as the gold standard in measurement methodology.

The 3D volume rendering CT technique allowed the raters to easily draw the proximal and distal tibial axes because of a well-defined identification of the anatomical landmark of interest on the tibial cortex. This observation may be relevant especially in the most complex cases of multiplanar deformities. We agree with Barnes et al[37] that some of the anatomical landmarks proposed in the current literature on TT[16,28] are challenging to be detected with the axial CT technique. First, the profile of the most prominent points of the tibial distocranial cortex may change across a range of breeds.[37] Second, it has not been previously defined which is the most appropriate slice of the transverse view of distal tibial epiphysis regarding where the CnT axis should be drawn.[28] When CT slices in a proximal-to-distal direction are scrolled through, the profile of the tibial distocranial prominences changes, thus influencing the CnT inclination. Barnes et al[37] used a distal "malleolar reference line" to bypass the problem related to the detection of distal tibial prominences.[37] However, the definition of TT implies the detection of intrinsic tibial landmarks. Therefore, we decided to use some of the previously reported tibial landmarks[28] but using an alternative CT methodology. The 3D volume rendering methodology allowed the raters to directly visualize the most prominent points of the distal cranial tibial cortex without needing to choose which was the most appropriate CT slice to draw the CnT axis.

One of the advantages of the 3D volume rendering function is that it allows the bone morphology to be freely manipulated in 3D space.[31,33,34] Several DICOM software packages provide a semitransparent bone filter as an additional tool to analyze 3D bone models.[32,38] This function offers a significant advantage compared with both axial CT and 3D volume rendering CT without a semitransparent filter because some anatomical landmarks may be undetectable when the proximal and distal epiphyses are superimposed. The bone transparency allows for the assessment of the regions of interest with the desired plane of view because it has been already described for the evaluation of radial,[38] femoral,[8,37] and tibial axial and frontal alignment.[32] The use of the 3D volume rendering function implemented with a semitransparent bone filter may be particularly helpful when complex tibial multiplanar deformities are evaluated. In cases with severe patella luxation, tibial torsion may often be detected along with other deformities such as tibial varus/valgus, pes deviation, or metatarsal rotation.[8,17,20] The simultaneous presence of these deformities may complicate the detection of anatomical landmarks, axis drawing, and angle measurements with both axial and 3D volume rendering CT techniques. Additional research in which both CT techniques are compared is warranted to determine whether the 3D volume rendering evaluation of tibiae affected by multiplanar deformities is superior to standard axial CT technique.

All three raters found that the 3D manipulation of the bone model was a great advantage of the 3D volume rendering CT technique as they performed the measurements, regardless of the initial bone positioning. Furthermore, the superimposition of the two reference points, used to find the frontal tibial mechanical axis, allowed the raters to use a consistent proximal-to-distal positioning during their measurements. This may partially explain the high accuracy and excellent precision found with the 3D volume rendering CT technique. The axial CT technique may be affected by a potential positioning artifact.[28] When the bone is not positioned orthogonal to the CT gantry, the angular relationship between the CdC and CnT changes because of the angular change between the tibia and the CT gantry. Furthermore, the plane of the CT slice would not be representative of the same tibial landmarks that have been used for the anatomic measurements.[28]

We accept our second hypothesis because an overall mean of approximately −6°of internal TT was found in dogs unaffected by patella luxation. This finding provides evidence that, in this group of dogs, the distal tibial epiphysis was slightly internally oriented compared with the proximal tibial epiphysis. Our results are also in agreement with the outcomes of the two studies that used the same pair of axes.[26,27] The comparison between reports of studies that have used CT for evaluating TT could be misleading, with some of them describing a physiological internal torsion[28,32] and others describing external torsion.[19,28-31] Explanations for this measurement discrepancy are primarily ascribable to the use of two different pairs of axes to calculate the same object (TTa; Figure 5, Table 4).[19,28-32,37] As a result, depending on which pair of axes was adopted, the angular value for TT changed. Second, we found an inconsistency concerning the criteria for assigning a negative or positive value to the angle measured. Aper et al[28] attributed negative and positive values depending on whether a clockwise or counter-clockwise offset was respectively found. In addition, the authors considered which tibia (left/

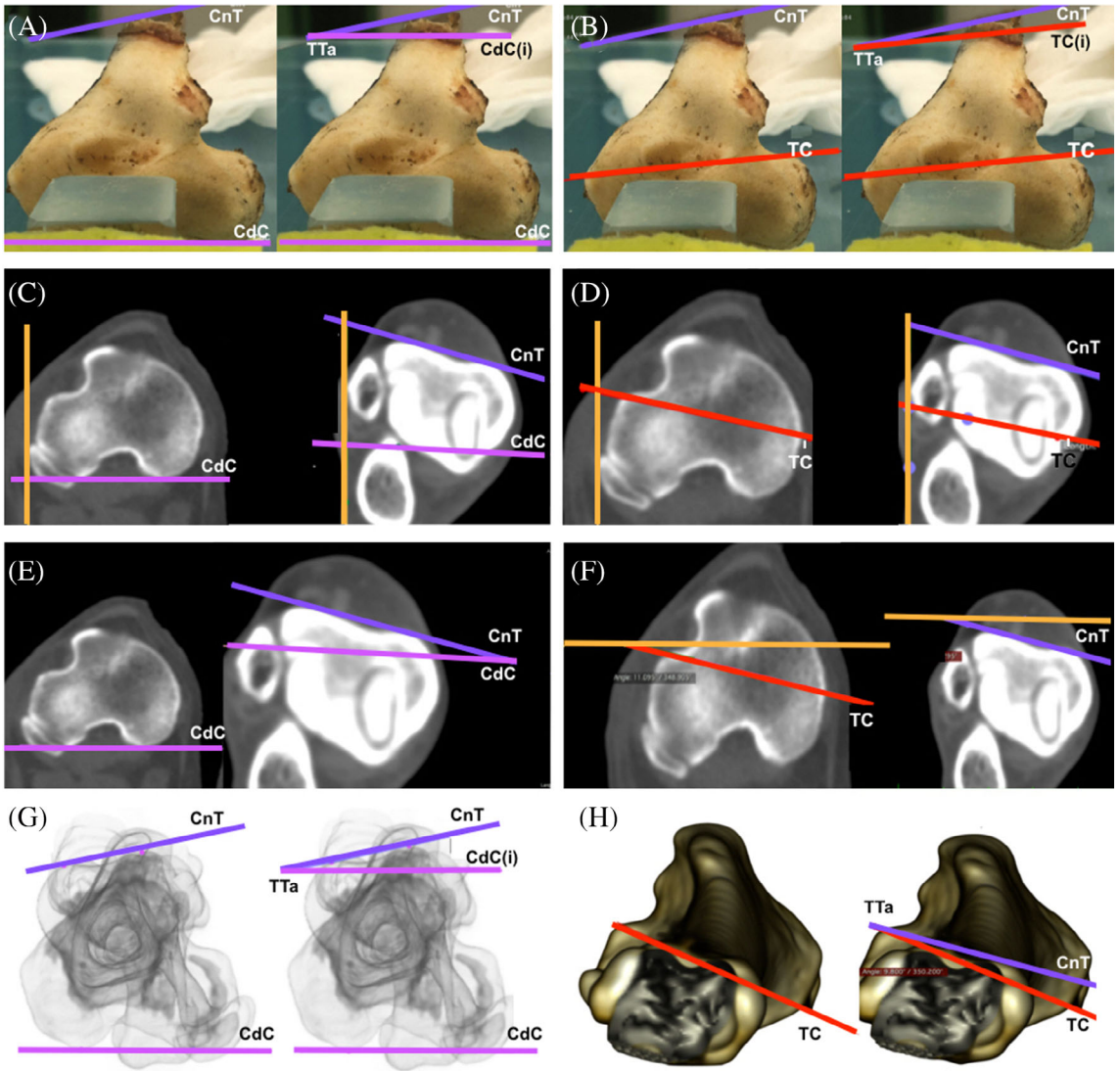

FIGURE 5 Evaluation of tibial torsion angle (TTa) by using anatomical, axial, and three dimensional computed tomography (3D CT) techniques in a right tibia of a Labrador retriever by using different reported methods.[19,28,31,32] The TTa was assessed by using either caudal condylar/cranial tibial (CdC/CnT) or transcondylar/cranial tibial (TC/CnT) pair of axes. A,B The anatomical measurement of TTa by using CdC/CnT axes (A, TTa: −12,4°) and TC/CnT axes (B, TTa: −7°). C,D The measurement of the TTa by using the axial CT with CdC/CnT axes (C, TTa: −11,6°) and the TC/CnT axes (D, TTa: −3.7°).[28] E, The measurement of TTa (−12°) with CdC/CnT axes by using the methodology presented by Newman et al.[32] F, The TTa measurement (− 0.6°) by using TC/CnT axes by using the methodology described by Fitzpatrick et al.[19] G, The TTa (−12°) is measured by using the 3D CT technique reported in this study. H, The TTa measurement (−9.8°) with TC/CnT axes, as reported by Yasukawa et al.[31]

TABLE 4 Reports of TTa measured with CT in canine breeds not affected by patella luxation

TT angle	Aper et al[28]	Newman and Voss[32]	Current study	Fitzpatrick et al[19]	Lusetti et al[29]	Yasukawa et al[31]	Phetkaew et al[30]
CdC/CnT, ° (breed)	−4.85 ± 5.19 (MB)	−4.51 ± 3.95 (BT)	−5.80 ± 5.70 (MB)	...	...	...	...
TC/CnT, ° (breed)	4.15 ± 6.05 (MB)	...	...	9.1 ± 4.1 (YK)	4.0 ± 8.82 (EB)	11.3 ± 4.3 (TP)	6.7 ± 3.2 (CH)

Note: Data are mean ± SD. Two pairs of axes were used: the proximal CdC/distal CnT axis or the proximal TC/CnT axis. Negative values = internal TT, and positive values = external TT.

Abbreviations: ..., not applicable; BT, bull terrier; CdC, caudal condylar; CH, Chihuahua; CnT, cranial tibial; EB, English bulldog; MB, multiple breeds; TC, transcondylar; TP, toy poodle; TTa, tibial torsion angle; YK, Yorkshire.

right) was examined. This implies that, in the case of an internal TT, a negative value was assigned to the left tibia and a positive value to the right tibia. Other researchers, by convention, assigned a negative value when an internal TT was found and a positive value to the external TT, regardless of the limb side.[19,29,30] To avoid any further ambiguity, in a proximal-to-distal axial view, we attributed a negative value when the vertex of the CdC/CnT angle was found medially (internal TT) and a positive value (external TT) when it was found in the lateral direction.

The findings of this study should be considered in light of some study limitations. We used a heterogeneous group of medium-to-large-sized dogs. Thus, unlike researchers in several other studies, we did not investigate TT in a single breed.[19,29-32] As a result, we could not provide a breed reference range. Furthermore, we did not include toy breeds. It is possible that toy breeds could be characterized by a physiological external TT, which was highlighted by the outcomes of some studies.[19,30,31] The mean value of internal TT found may have been mitigated by the heterogeneity of tibiae evaluated. Second, it is possible that this study was not adequately powered to provide evidence of a difference that actually existed among the considered variables. Thus, the presence of a type II statistical error could not be completely excluded. With a 3.5° difference between CT and anatomic measurements, 36 samples were enough to assure statistical power of 82%.

In the axial CT technique, the tibia was oriented only according to the frontal plane, so we may not have been as consistent with positioning as we were with the 3D volume rendering technique. The use of the 3D MPR function would have been a reliable option for better orienting the tibia. Finally, only one additional examiner performed the measurements on the digital images of the anatomic specimens, and this may have eventually led to a more uniform data set for the anatomical model measurements.

In conclusion, evaluating TT by using 3D reconstructed CT images is a reliable alternative to the previously described axial CT technique. The 3D volume rendering CT methodology exhibited excellent precision and accuracy. The evaluation of torsional deformity by using a 3D bone model, assessed through a semitransparent filter, allows the rater to position the bone in a true axial plane, with the main advantage of being able to detect all the required anatomical landmarks simultaneously.

A physiological internal TT of −6° was found in dogs unaffected by patella luxation. Although this outcome was in agreement with the results of some publications, the present study could not confirm whether these findings could be suggested as reference values for a large canine population. Additional TT assessments with the same methodology must be performed in target canine breeds that are commonly affected by patella luxation.

ACKNOWLEDGMENTS

Author contributions: Longo F, DVM, PhD: Designed the study, performed the measurements, analyzed and interpreted the data, drafted the manuscript, and read and approved the final manuscript; Nicetto T, DVM, PhD: Participated in the design of the study, performed the measurements, interpreted the data, and read and approved the final manuscript; Pozzi A, DVM, ACVS, ECVS, ACVSMR: Participated in the design of the study, interpreted the data, revised the manuscript, and read and approved the final manuscript; Contiero B, MsS: Performed statistical analysis, analyzed the data, and read and approved the final manuscript; Isola M, DVM, PhD: Performed the measurements, interpreted the data, revised the manuscript, and read and approved the final manuscript.

CONFLICT OF INTEREST

The authors declare no conflicts of interest related to this study.

ORCID

Federico Longo https://orcid.org/0000-0002-3396-4768

REFERENCES

1. Dismukes DI, Fox DB, Tomlinson JL, Cook JL, Essman SC. Determination of pelvic limb alignment in the large-breed dog: a cadaveric radiographic study in the frontal plane. *Vet Surg.* 2008;37:674-682.
2. Paley D. Growth plate consideration. In: Paley D, Herzenberg JE, eds. *Principles of Deformity Correction*. Berlin, Germany: Springer-Verlag; 2005:703-710.
3. Ramadan RO, Vaughan LC. Disturbance in the growth of the tibia and femur in dogs. *Vet Rec.* 1979;104:433-435.
4. Reikeras O, Kristiansen LP, Gunderson R, Steen H. Reduced tibial torsion in congenital clubfoot: CT measurements in 24 patients. *Acta Orthop Scand.* 2001;72:53-56.
5. von Pfeil DJ, DeCamp CE, Abood SK. The epiphyseal plate: nutritional and hormonal influences; hereditary and other disorders. *Compend Contin Educ Vet*. 2009;31:E1-E13; quiz E14.
6. Prasad CV, Khalid M, McCarthy P, O'Sullivan ME. CT assessment of torsion following locked intramedullary nailing of tibial fractures. *Injury.* 1999;30:467-470.
7. Crosse KR, Worth AJ. Computer-assisted surgical correction of an antebrachial deformity in a dog. *Vet Comp Orthop Traumatol.* 2010;23:354-361.
8. DeTora MD, Boudrieau RJ. Complex angular and torsional deformities (distal femoral malunions). Preoperative planning using stereolithography and surgical correction with locking plate fixation in four dogs. *Vet Comp Orthop Traumatol.* 2016;29:416-425.
9. Holt K, Boettcher C, Halaki M, Ginn KA. Humeral torsion and shoulder rotation range of motion parameters in elite swimmers. *J Sci Med Sport.* 2017;20:469-474.
10. Leonardi F, Rivera F, Zorzan A, Ali SM. Bilateral double osteotomy in severe torsional malalignment syndrome: 16 years follow-up. *J Orthop Traumatol.* 2014;15:131-136.
11. Longo F, Penelas A, Gutbrod A, Pozzi A. Three-dimensional computer-assisted corrective osteotomy with a patient-specific surgical guide for an antebrachial limb deformity in two dogs. *Schweiz Arch Tierheilkd.* 2019;161:473-479.
12. Bouchard R, Meeder PJ, Krug F, Libicher M. Evaluation of tibial torsion - Comparison of clinical methods and computed tomography. *Rofo.* 2004;176:1278-1284.
13. Güven M, Akman B, Ünay K, Özturan EK, Çakıcı H, Eren A. A new radiographic measurement method for evaluation of tibial torsion: a pilot study in adults. *Clin Orthop Relat Res.* 2009;467:1807-1812.
14. Petazzoni M. Radiographic measurements of the tibia. In: Petazzoni M, Jaeger GH, eds. *Atlas of Clinical Goniometry and Radiographic Measurements of the Canine Pelvic Limb*. 2nd ed. Milano, Italy: Merial; 2008:60-71.
15. Clementz BG. Assessment of tibial torsion and rotational deformity with a new fluoroscopic technique. *Clin Orthop Relat Res.* 1989;(245):199-209.
16. Milner CE, Soames RW. A comparison of four in vivo methods of measuring tibial torsion. *J Anat.* 1998;193:139-144.
17. Dunlap AE, Kim SE, Lewis DD, Christopher SA, Pozzi A. Outcomes and complications following surgical correction of grade IV medial patellar luxation in dogs: 24 cases (2008-2014). *J Am Vet Med Assoc.* 2016;249:208-213.
18. Apelt D, Kowaleski MP, Dyce J. Comparison of computed tomographic and standard radiographic determination of tibial torsion in the dog. *Vet Surg.* 2005;34:457-462.
19. Fitzpatrick CL, Krotscheck U, Thompson MS, Todhunter RJ, Zhang Z. Evaluation of tibial torsion in Yorkshire Terriers with and without medial patellar luxation. *Vet Surg.* 2012;41:966-972.
20. Johnson SG, Hulse DA, Vangundy TE, Green RW. Corrective osteotomy for pes varus in the dachshund. *Vet Surg.* 1989;18:373-379.
21. Borish CN, Mueske NM, Wren TAL. A comparison of three methods of measuring tibial torsion in children with myelomeningocele and normally developing children. *Clin Anat.* 2017;30:1043-1048.
22. Shin SY, Yoon CH, Lee ES, et al. The availability of radiological measurement of tibial torsion: three-dimensional computed tomography reconstruction. *Ann Rehabil Med.* 2011;35:673-679.
23. Panou A, Stanitski DF, Stanitski C, Peccati A, Portinaro NM. Intra-observer and inter-observer errors in CT measurement of torsional profiles of lower limbs: a retrospective comparative study. *J Orthop Surg Res.* 2015;10:67.
24. Sangeux M, Mahy J, Graham HK. Do physical examination and CT-scan measures of femoral neck anteversion and tibial torsion relate to each other? *Gait Posture.* 2014;39:12-16.
25. Liodakis E, Doxastaki I, Chu K, et al. Reliability of the assessment of lower limb torsion using computed tomography: analysis of five different techniques. *Skeletal Radiol.* 2012;41:305-311.
26. Hudson D, Royer T, Richards J. Ultrasound measurements of torsions in the tibia and femur. *J Bone Joint Surg Am.* 2006;88:138-143.
27. Clementz BG. Fluoroscopy of rotation in tibial fractures. *Acta Orthop Scand.* 1989;60:204-207.
28. Aper R, Kowaleski MP, Apelt D, Drost WT, Dyce J. Computed tomographic determination of tibial torsion in the dog. *Vet Radiol Ultrasound.* 2005;46:187-191.
29. Lusetti F, Bonardi A, Eid C, de Bellesini AB, Martini FM. Pelvic limb alignment measured by computed tomography in purebred English Bulldogs with medial patellar luxation. *Vet Comp Orthop Traumatol.* 2017;30:200-208.
30. Phetkaew T, Kalpravidh M, Penchome R, Wangdee C. A comparison of angular values of the pelvic limb with normal and medial patellar luxation stifles in Chihuahua dogs using radiography and computed tomography. *Vet Comp Orthop Traumatol.* 2018;31:114-123.
31. Yasukawa S, Edamura K, Tanegashima K, et al. Evaluation of bone deformities of the femur, tibia, and patella in Toy Poodles with medial patellar luxation using computed tomography. *Vet Comp Orthop Traumatol.* 2016;29:29-38.
32. Newman M, Voss K. Computed tomographic evaluation of femoral and tibial conformation in English Staffordshire Bull Terriers with and without congenital medial patellar luxation. *Vet Comp Orthop Traumatol.* 2017;30:191-199.
33. Longo F, Nicetto T, Banzato T, et al. Automated computation of femoral angles in dogs from three-dimensional computed tomography reconstructions: comparison with manual techniques. *Vet J.* 2018;232:6-12.
34. Oxley B, Gemmill TJ, Pink J, et al. Precision of a novel computed tomographic method for quantification of femoral varus in dogs and an assessment of the effect of femoral malpositioning. *Vet Surg.* 2013;42:751-758.

35. Dismukes DI, Tomlinson JL, Fox DB, Cook JL, Song KJ. Radiographic measurement of the proximal and distal mechanical joint angles in the canine tibia. *Vet Surg*. 2007;36:699-704.
36. Longo F, Savio G, Contiero B, et al. Accuracy of an automated three-dimensional technique for the computation of femoral angles in dogs. *Vet Rec*. 2019;185(14):443.
37. Barnes DM, Anderson AA, Frost C, Barnes J. Repeatability and reproducibility of measurements of femoral and tibial alignment using computed tomography multiplanar reconstructions. *Vet Surg*. 2015;44:85-93.
38. Kroner K, Cooley K, Hoey S, Hetzel SJ, Bleedorn JA. Assessment of radial torsion using computed tomography in dogs with and without antebrachial limb deformity. *Vet Surg*. 2017;46:24-31.

How to cite this article: Longo F, Nicetto T, Pozzi A, Contiero B, Isola M. A three-dimensional computed tomographic volume rendering methodology to measure the tibial torsion angle in dogs. *Veterinary Surgery*. 2021;50:353–364. https://doi.org/10.1111/vsu.13531